Large Eddy Simulation of Isothermal and Non-isothermal Turbulent Flows in Ventilated Classrooms

Ramesh Balakrishnan[1], Rao Kotamarthi[1] and Paul Fischer[2]

[1] *Argonne National Laboratory, Argonne IL 60439*
[2] *University of Illinois at Urbana-Champaign, Urbana, IL 61801*

bramesh@anl.gov

Abstract

In this paper we present results from a full resolved large eddy simulations (LES) of a modified Nielsen [10] test case, and a newly designed model classroom, with different arrangements of student units and ventilation pathways. The results of our LES indicate that we are able to capture the flow physics in the high Reynolds number jet region (*i.e.* the region along the direction where the flow enters the room via the ventilation ducts), resolve the regions of the flow near the solid wall surfaces, and simulate the effects of temperature gradients on the flow. We also demonstrate that despite the fact that the number of grid points required for a fully resolved LES is higher than the meshing requirements for Reynolds Averaged Navier-Stokes (RANS) simulations, our computational framework, which consists of a higher-order (highly scalable) spectral element code, makes it possible to use LES as an effective design tool.

1 Introduction

Since the discovery of the SARS-CoV-2 virus, and the ensuing COVID-19 pandemic, we have come to understand that the rule-of-thumb guidelines for *social distancing* (about six-feet) between people, is at best a crude estimate [1] for an outdoor environment, and in the absence of any prevailing wind. In an enclosed environment, however, as evidenced by the outbreak of COVID-19 in an indoor restaurant in Guangzhou, China (in January 2020), it has been suggested [8] that the spread of the disease was due to build-up of droplets and aerosols (that had carried the SARS-CoV-2 virus), despite the fact that the restaurant was ventilated and the people in the restaurant were reasonably social-distanced from each other, when seated around the table. This case motivates the need for understanding the complex flow physics, and the effects of temperature and flow turbulence on the migration and preferential accumulation of aerosol particles of size $[0.5, 15.0]\,\mu$m, that are exhaled by people during normal breathing and speaking. Over the last year, therefore, there has been renewed interest in simulating flows-particle interactions in enclosed spaces, in order to assess the length of time for which aerosol particles continue to remain in a ventilated room, and to estimate the deposition of aerosol particles in the neighborhood of people in a room.

Ventilated rooms are marked by flows that are unsteady (with regions of separated and recirculating flows), and contain intermittent *dead-zones* where the flow has very low velocity and turbulent kinetic energy (TKE). Flows in classrooms, in particular, are also marked by the fact that students create islands (discrete regions) in the room with fairly large local temperature gradients (due to their body temperature being higher than the ambient temperature), and local aerosol concentration gradients (due to the aerosols that are emitted when they breathe/speak), that adds more complexity of the flow. Due to the computational cost of doing resolved simulations of the flow-field, which is inherently unsteady, the vast majority of flow simulations in enclosed spaces has been with RANS models (with known limitations for predicting separated and recirculating flows), and LES on coarse meshes [13] with very diffusive subgrid scale (SGS) models. In particular, the use of RANS for simulating such flows leads to poor (and even incorrect) predictions of the effects of temperature and flow turbulence on the dispersion and deposition of aerosol particles. Further, the paucity of high resolution experimental data, with very limited statistical information about the velocity and temperature fluctuations in an enclosed space makes it difficult to assess (and improve) RANS models, to predict quantities of interest in *what-if* scenarios rapidly and reliably (with quantification of the uncertainties). There is a need, therefore, for a computational capability for using LES, to design newer experiments of flows in enclosed spaces (with improved measurements of turbulence statistics), and to also serve as a design tool (to inform HVAC manufacturers and building engineers).

The goal of our research, therefore, was two fold: *i.)* to advance our understanding of turbulent flows in enclosed rooms, and to inform the development of new experiments, via well-resolved large eddy simulations of isothermal and non-isothermal flows at re-

alistic ventilation flow rates, and *ii.)* to demonstrate LES as a viable tool for designing indoor ventilation systems, by exploring the parameter space via ensemble simulations on heterogeneous computing (*i.e.* CPU+GPU) platforms. In our study, we have considered isothermal and non-isothermal flows in a modified Nielsen test case, and a model classroom, with different ventilation patterns (by changing the location of HVAC vents), and changes to the layout of student units in the classroom.

2 Methodology

To model the turbulent flow in a ventilated room, we solve the incompressible Navier-Stokes equation, modified by the addition of a buoyancy force term (via the Boussinesq approximation), and the temperature equation, together with the continuity equation to ensure that the velocity field is divergence free. The governing equations are given by:

$$\frac{\partial \mathbf{u}}{\partial t} + \mathbf{u}\cdot\nabla\mathbf{u} = -\frac{1}{\rho_0}\nabla P + \nu\nabla^2\mathbf{u} - \beta(T-T_0)\mathbf{g} \quad (1)$$

$$\frac{\partial T}{\partial t} + \mathbf{u}\cdot\nabla T = \frac{\lambda}{\rho_0 c_p}\nabla^2 T \quad (2)$$

$$\nabla\cdot\mathbf{u} = 0 \quad (3)$$

where $\mathbf{u}$ is the velocity, T is the temperature, P is the pressure, ρ_0 and T_0 are the density and temperature of the undisturbed fluid (air), respectively, β is the coefficient of thermal expansion, c_p is the heat capacity of the fluid, and λ is the thermal conductivity of the fluid. For isothermal flow simulations we only evolve equation (1) with the continuity constraint (3).

The governing equations are evolved using the higher-order (highly scalable) spectral element code, Nek5000, and the newer GPU enabled nekRS spectral element code. The Nek5000/nekRS codes [11, 2] are based on a high-order spectral element method (SEM) in which the solution is represented with pth-order tensor-product polynomial bases in each of E elements, for a total of $n \approx Ep^3$ grid points in the domain. Typical values of p are 5–9, with $p = 7$ being the most common choice. These methods are exponentially convergent in p, which means that numerical dispersion is minimal for all resolved modes (i.e., all modes, in the case of DNS). We use the $\mathcal{P}_n - \mathcal{P}_n$ formulation, which means that P and $\mathbf{u}$ are collocated on the Gauss-Lobatto-Legendre (GLL) points, and are represented by basis functions of the same polynomial order. The nonlinear term is fully dealiased which ensures that the eigenvalues of the transport operator are imaginary and that method is therefore stable for any timestepper whose stability region encompasses the imaginary axis near the origin, as in the present case [9]. Navier-Stokes time advancement uses 3rd-order BDF/extrapolation in time, with explicit treatment of the nonlinear term and independent system solves for the viscous and pressure updates. The viscous systems are diagonally dominant and require only a few iterations of Jacobi-preconditioned conjugate gradients for each step. The pressure solve uses p-multigrid with overlapping Schwarz smoothing [4, 5]. For the coarsest level, we use the AMG solver that is in Nek5000's *gslib* package, which is specifically tuned this class of problems with minimal communication overhead [5, 3]. In sharp contrast to the the p-type finite element method, which has $O(Ep^6)$ complexity, the storage for the SEM scales as n, independent of p, while the leading-order work term scales as $np = Ep^4$. Moreover, the SEM features a communication-minimal stencil depth of unity, independent of p. All the $O(p^4)$ terms can be cast as dense matrix-matrix products involving tensor contractions with $O(p\times p)$ operators applied to $O(p^3)$ data for each element, in parallel. On Summit V100s, the principal work kernels are realizing 1–2 Tflops (fp64) by leveraging the libParanumal library of Warburton and co-workers [6, 12].

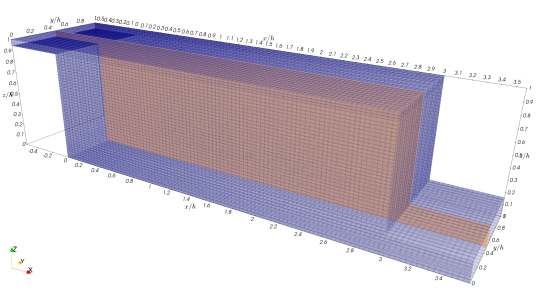

Figure 1: Volume mesh for the isothermal and non-isothermal simulations of the Nielsen experiment [10] and the modified Nielsen case.

3 Results

Nielsen Experiment

In order to demonstrate the highly accurate jet and wall resolved LES flows fields obtained from spectral element based LES, we simulated the Nielsen experiment [10], with the flow conditions as in [7], and also extended this test case (modified Nielsen case) for non-isothermal flows. For the isothermal and non-isothermal cases, the domain was meshed as shown in Fig. 1. Two sets of meshes were used, with the finer mesh consisting of approximately double the number of GLL points, in order to ensure that the mean flow solutions (for the isothermal flow case) were mesh converged. The mesh consisted of 85491 hexahedral elements, with seventh-order and ninth-order polynomial as the basis functions for the flow variables. For the isothermal case, the simulations were averaged over 400 flow through times.

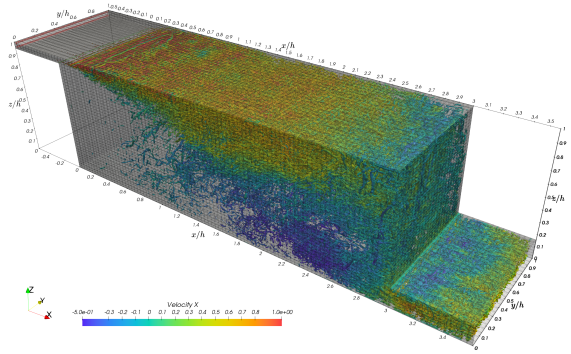

(a)

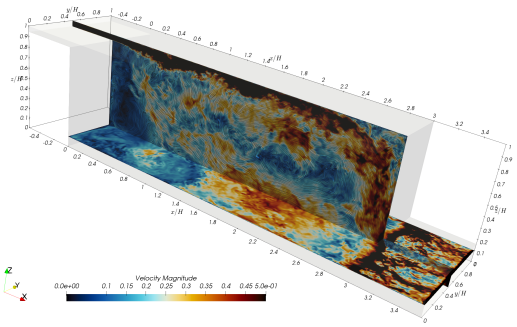

(b)

Figure 2: Isothermal Simulation results for the Nielsen experiment [10]. (a): λ_2 isosurface colored by velocity, (b) velocity contours indicate the dead-zone in the front of the room.

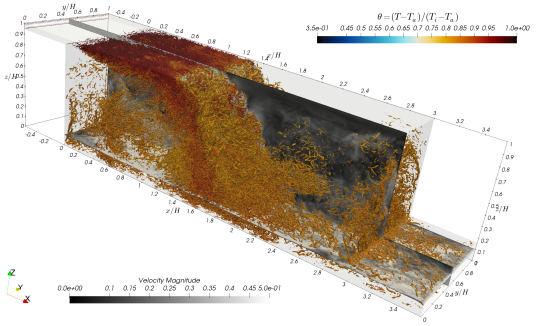

(a)

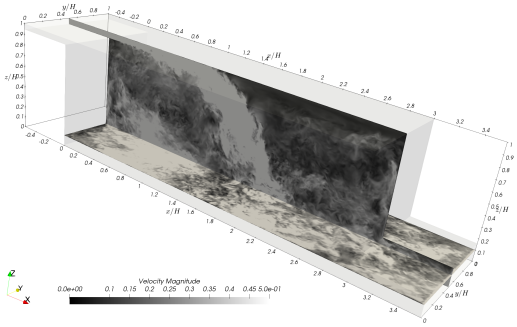

(b)

Figure 3: Non-isothermal results with the inlet temperature 5^o Celsius cooler than the ambient. (a): λ_2 isosurface colored by θ, and (b) note the reduction in the extent of the dead-zone in the front of the room.

Figures 2a and 2b show the λ_2 iso-surfaces, colored by velocity, and a contour plot of the velocity on the mid plane, and on a plane just above the floor of the room. Since the flow comes in from an inlet on the top left wall of the room, and exits from an outlet on the bottom right wall of the room, we note the formation of a large dead-zone near the inlet wall where the flow is almost stagnant. In order to consider the transient effects of cooling and heating we considered two cases that were each initialized with the velocity field obtained from the isothermal case. In the first of these two additional cases, the temperature of the incoming air was colder than the ambient by 5^o Celsius, and in the second case, the incoming air was hotter than the ambient air by 5^o Celsius. For these non-isothermal cases, temperature boundary conditions were applied by: a) considering the walls of the room to be insulated (*i.e.* adiabatic, with $dT/dn = 0$), b) specifying the incoming jet temperature at the inlet (Dirichlet BC), and c) setting the temperature gradient $dT/dx = 0$ at the outlet boundary (similar to the velocity BC). We evolved the simulation for one flow through time, to mimic the flow and temperature transients in the classroom, after which the HVAC unit is assumed to cut out after the room temperature reaches a preset value.

An important point to note from figures 3, and 4 is that the extent of the dead-zone, near the inlet wall, is decreased when the incoming jet is cooler than the ambient (fig. 3). This is due to the fact that the cooler incoming air jet is less buoyant, and creates a strong downward flow near the inlet wall region, thereby pushing the dead zone closer to the inlet wall. Further reduction in the temperature of the incoming air causes the dead-zone to disappear.

However, when the incoming air is hotter than the ambient, it is more buoyant and tends to stay in the upper regions of the room, thereby creating a stratification layer that reduces the turbulence intensity in the room. As a result, the dead-zone extends further away from the inlet wall when the incoming jet is hotter (fig. 4).

Model Classroom

To simulate flows in a model classroom, we designed a layout consisting of student units arranged in 5×5 matrix layout, and a staggered layout, where every alternate student unit was removed. The dimensions of the model classroom has a height of 3 meters, and length and width of 14 and 12 meters, respectively. The student units, which represents the space occupied by a seated student, together with

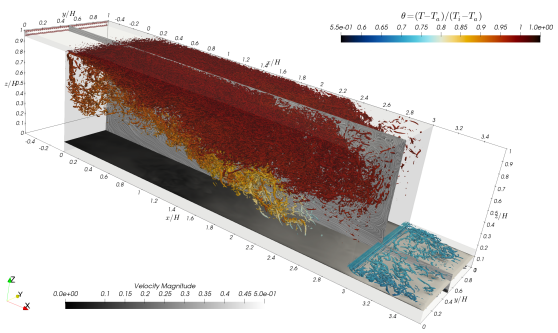

(a)

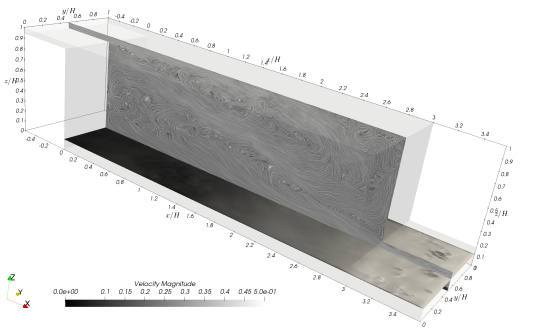

(b)

Figure 4: Non-isothermal results with the inlet temperature 5^o Celsius hotter than the ambient.(a): λ_2 isosurface colored by θ, and (b) note the increase in the extent of the dead-zone in the front of the room.

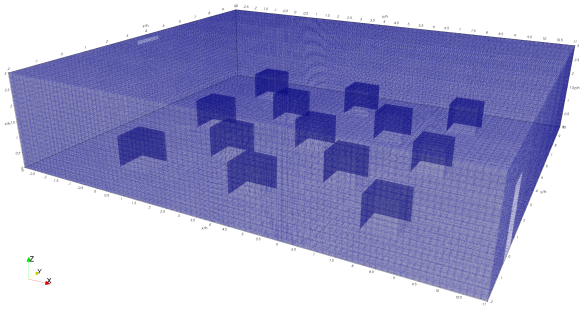

(a)

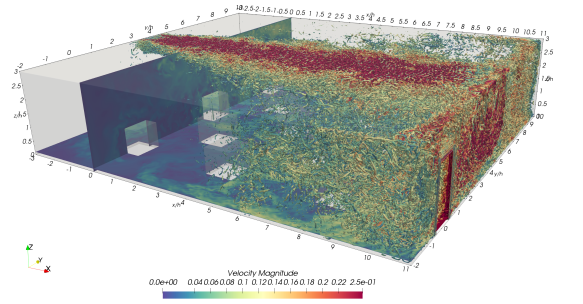

(b)

Figure 5: Staggered layout of student units. (a): spectral element mesh of the model classroom, and (b): λ_2 structures and velocity contours suggest a dependence of the extent of the dead-zone on the Reynolds number.

the desk and chair is considered to be a $1 \times 1 \times 1m^3$ unit, and with a realistic flow rate that ranges from $[0.3, 0.6]$ m^3/sec, a jet velocity that ranges from $[1, 2]$ m/sec, and temperature variations of $\pm 20^o$ Celsius. The air flow rate in the model classroom corresponds to the ASHRAE recommended air changes per hour (ACH) of $ACH = 3$. The Reynolds number of the flow in the model classroom is in the range of $[10^5, 2 \times 10^5]$, based on the height of the student unit. As a result, these simulations are at a higher Reynolds number than that of the Nielsen experiment, and are considerably more expensive.

While the effects of temperature stratification in the model classroom layouts are similar (qualitatively speaking) to the results of the modified Nielsen case, there are additional dead-zones that are created in the space between the student units, where pathogen laden aerosols can build up and remain trapped. Interestingly, for the case of isothermal flow in a model classroom with a matrix layout (fig. 8), we note that the arrangement of the HVAC inlet and the door of the classroom on the same wall appears to prevent the formation of dead-zones.

4 Conclusions

We have carried out LES that fully resolve the incoming jet of air, for isothermal and non-isothermal flows in the Nielsen experiment and modified Nielsen case, respectively. The isothermal simulation results for the Nielsen experiment compare well with [7], and serve as a reference to understand the effects of buoyancy on the turbulence in a ventilated room. The non-isothermal simulations on the modified Nielsen case highlight the effect of temperature stratification on the ambient turbulence levels, and, in particular, on extent of the dead zones.

The simulations of the model classroom were carried out for two different Reynolds numbers (based on the inlet velocity and the height of the student unit) together with combinations of the layout of the student units and ventilation pathways. Care was taken to ensure that the mesh resolution used for our simulations resolved the flow in the incoming jet as well as the flow over the walls of the room, and the other solid wall surfaces therein. While the effect of temperature on the flow turbulence is qualitatively similar to that of the modified Nielsen case (and has, therefore, not been reported in this paper), this case allowed us to explore strategies for directing the flow in a manner that nullifies the formation of dead-zones. Further, the individual cases in the test matrix for the model classroom, constituted an ensemble of simulations on Summit, a heterogeneous computing platform at Oak Ridge National Labora-

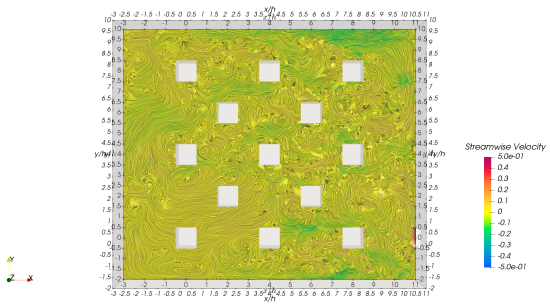

(a)

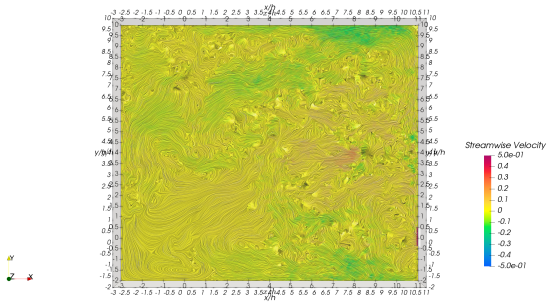

(b)

Figure 6: Streamwise velocity plots on two different horizontal planes. (a): contours on a plane at the height of the student unit ($z = 1.0$), and (b): contours on the mid-plane ($z = 1.5$).

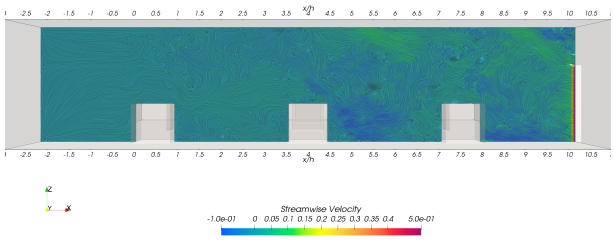

(a)

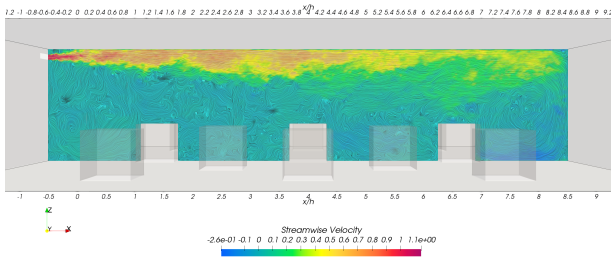

(b)

Figure 7: Streamwise velocity plots on two different vertical planes. (a): contours on a plane close to the walls ($y = 0.0$), and (b): contours on the mid-plane ($y = 0.0$).

tory. The use of the highly scalable Nek5000/nekRS spectral element code for our simulations point to the viability of using fully resolved LES as a design tool for developing HVAC units for enclosed spaces, such as offices and classrooms.

In this paper, our aim has been on understanding the physics of isothermal and buoyant turbulent flows in enclosed ventilated spaces, and on the location and extent of dead zones. These intermittent regions of low fluid velocity and TKE, are important because the small aerosols ($\approx 1.0 - 5.0\mu$m) that are either released within, or migrate to, these zones, could linger in the room for much longer periods of time. If these aerosol particles, that accumulate preferentially in these dead zones, were to contain a high virion density, the enclosed space as a whole could become infected. Hence, it is necessary to understand the conditions under which dead-zones form, and to devise strategies for improving the ventilation, in order to mitigate the risk of airborne infection. While increasing the ACH is an effective means of flushing out airborne pathogens, such as the SARS-Cov-2 virus, the means for doing this in classrooms could be prohibitively expensive; especially in winter, when it is impossible (in colder countries) to exploit natural cross ventilation (by opening the windows) to increase the ACH. As a result, we need to be clever about designing new classrooms, and modifying existing classrooms, to increase the ACH in a cost effective manner. In the model classroom simulations that have been presented, we have explored one such solution, which was to move the exit of the classroom from the wall opposite the inlet wall, to the wall that houses the HVAC inlet. With the computational capability that we have developed, other cost effective design modifications to prevent the formation of dead zones are being explored, and simulations of coupled flow-particle interactions to understand the effects of thermal stratification on the dynamics of aerosols are currently underway.

5 Acknowledgment

This research was supported at the Argonne National Laboratory by the DOE Office of Science through the National Virtual Biotechnology Laboratory, a consortium of DOE National Laboratories focused on response to COVID-19, with funding provided by the Coronavirus CARES Act. This research used resources of the National Energy Research Scientific Computing Center (NERSC), a U.S. Department of Energy Office of Science User Facility located at Lawrence Berkeley National Laboratory, operated under Contract No. DE-AC02-05CH11231. This research also used resources of the Oak Ridge Leadership Computing Facility at the Oak Ridge Na-

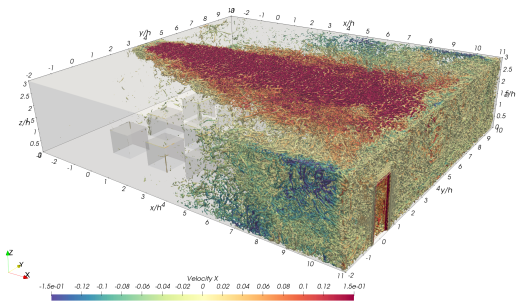

(a)

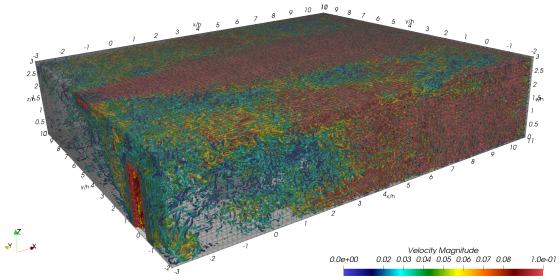

(b)

Figure 8: Isothermal results showing the λ_2 structures for a matrix layout. (a): ventilation jet and room exit, on opposite sides of the room, and (b): ventilation jet and room exit on the same wall. A change in the ventilation pathway appears to prevent the formation of the dead-zone seen in a).

tional Laboratory, which is supported by the Office of Science of the U.S. Department of Energy under Contract No. DE-AC05-00OR22725. Finally, we gratefully acknowledge the computing resources provided on Bebop, a high-performance computing cluster operated by the Laboratory Computing Resource Center at Argonne National Laboratory.

6 References

[1] M. Abuhegazy, K. Talaat, O. Anderoglu, and S. V. Poroseva. Numerical investigation of aerosol transport in a classroom with relevance to covid-19. *Physics of Fluids*, 32:103311, 2020.

[2] P. Fischer. *Spectral element solution of the Navier-Stokes equations on high performance distributed-memory parallel processors*. PhD thesis, Massachusetts Institute of Technology, 1989. Cambridge, MA.

[3] P. Fischer, K. Heisey, and M. Min. Scaling limits for PDE-based simulation (invited). In *22nd AIAA Computational Fluid Dynamics Conference, AIAA Aviation*. AIAA 2015-3049, 2015.

[4] P. Fischer and J. Lottes. Hybrid Schwarz-multigrid methods for the spectral element method: Extensions to Navier-Stokes. In R. Kornhuber, R. Hoppe, J. Périaux, O. Pironneau, O. Widlund, and J. Xu, editors, *Domain Decomposition Methods in Science and Engineering Series*. Springer, Berlin, 2004.

[5] P. Fischer, J. Lottes, W. Pointer, and A. Siegel. Petascale algorithms for reactor hydrodynamics. *J. Phys. Conf. Series*, 125:012076, 2008.

[6] P. Fischer, M. Min, T. Rathnayake, S. Dutta, T. Kolev, V. Dobrev, J.-S. Camier, M. Kronbichler, T. Warburton, K. Swirydowicz, and J. Brown. Scalability of high-performance PDE solvers. *IJHPCA*, in press, 2020.

[7] T. Foat, S. Parker, I. Castro, and Z.-T. Xie. Numerical investigation into the structure of scalar plumes in a simple room. *J. of Wind Engineering and Industrial Aerodynamics*, 175:252–263, 2018.

[8] J. Lu, J. Gu, K. Li, C. Xu, W. Su, Z. Lai, D. Zhou, C. Yu, B. Xu, and Z. Yang. Covid-19 outbreak associated with air conditioning in restaurant, guangzhou, china, 2020. *Emerging Infectious Diseases*, 26:1628–1631, 2020.

[9] J. Malm, P. Schlatter, P. Fischer, and D. Henningson. Stabilization of the spectral-element method in convection dominated flows by recovery of skew symmetry. *J. Sci. Comp.*, 57:254–277, 2013.

[10] P. V. Nielsen, A. Restivo, and J. H. Whitelaw. The velocity characteristics of ventilated rooms. *Journal of Fluids Engineering*, 100:291–298, 1978.

[11] A. Patera. A spectral element method for fluid dynamics : laminar flow in a channel expansion. *J. Comput. Phys.*, 54:468–488, 1984.

[12] K. Świrydowicz, N. Chalmers, A. Karakus, and T. Warburton. Acceleration of tensor-product operations for high-order finite element methods. *Int. J. of High Performance Comput. App.*, 33(4):735–757, 2019.

[13] V. Vuorinen, M. Aarnio, M. Alavah, V. Alopaeus, N. Atanasova, M. Auvinen, N. Balasubramanian, H. Bordbar, P. Erästö, R. Grande, N. Hayward, A. Hellsten, S. Hostikka, J. Hokkanen, O. Kaario, A. Karvinen, I. Kivistö, M. Korhonen, R. Kosonen, J. Kuusela, S. Lestinen, E. Laurila, H. J. Nieminen, P. Peltonen, J. Pokki, A. Puisto, P. Råback, H. Salmenjoki, T. Sironen, and M. Österbergd. Modelling aerosol transport and virus exposure with numerical simulations in relation to SARS-CoV-2 transmission by inhalation indoors. *Safety Science*, 130, 2020.